

Stress-Induced Apoptosis in *Spodoptera frugiperda* (Sf9) Cells: Baculovirus p35 Mitigates eIF2 α Phosphorylation[†]

Gunda Aparna,[‡] Abani K. Bhuyan,[§] Sudhir Sahdev,^{||} Seyed E. Hasnain,^{||,‡,¶} Randal J. Kaufman,[△] and Kolluru V. A. Ramaiah^{*,‡}

Department of Biochemistry and School of Chemistry, University of Hyderabad, Hyderabad 500 046, India, Laboratory of Molecular and Cellular Biology, CDFD, Nacharam, Hyderabad 500 076, India, National Institute of Immunology, New Delhi 110 067, India, JNCASR, Bangalore, India, and Department of Biological Chemistry, Howard Hughes Medical Institute, University of Michigan Medical Center, Ann Arbor, Michigan 48109

Received June 2, 2003; Revised Manuscript Received November 3, 2003

ABSTRACT: *Spodoptera frugiperda* (Sf9) ovarian cells, natural hosts for baculovirus, are good model systems to study apoptosis and also heterologous gene expression. We report that uninfected Sf9 cells readily undergo apoptosis and show increased phosphorylation of the α subunit of eukaryotic initiation factor 2 (eIF2 α) in the presence of agents such as UVB light, etoposide, high concentrations of cycloheximide, and EGTA. In contrast, tunicamycin, A23187, and low concentrations of cycloheximide promoted eIF2 α phosphorylation in Sf9 cells but without apoptosis. These findings therefore suggest that increased eIF2 α phosphorylation does not always necessarily lead to apoptosis, but it is a characteristic hallmark of stressed cells and also of cells undergoing apoptosis. Cell death induced by the above agents was abrogated by infection of Sf9 cells with wild-type (wt) AcNPV. In contrast, Sf9 cells when infected with vAc δ 35, a virus carrying deletion of the antiapoptotic p35 gene, showed increased apoptosis and enhanced eIF2 α phosphorylation. Further, a recombinant wt virus vAcS51D expressing human S51D, a phosphomimetic form of eIF2 α , induced apoptosis in UVB pretreated Sf9 cells. However, infection with vAcS51A expressing a nonphosphorylatable form (S51A) of human eIF2 α partially reduced apoptosis. Consistent with these findings, it has been observed here that caspase activation has led to increased eIF2 α phosphorylation, while caspase inhibition by z-VAD-fmk reduced eIF2 α phosphorylation selectively in cells exposed to proapoptotic agents. These findings therefore suggest that the stress signaling pathway determines apoptosis, and caspase activation is a prerequisite for increased eIF2 α phosphorylation in Sf9 cells undergoing apoptosis. The findings also reinforce the conclusion for the first time that the “pancaspase inhibitor” baculovirus p35 mitigates eIF2 α phosphorylation.

Changes in gene expression at the translational level occur in eukaryotic cells in response to a wide variety of conditions that are known to promote or inhibit cell growth, cell transformation, and programmed cell death. Eukaryotic initiation factor 2 (eIF2), a key regulatory protein involved in polypeptide chain initiation, is a heterotrimer with three subunits: α , β , and γ . It facilitates the joining of initiator tRNA (Met-tRNA_i) to the 40S ribosomal subunit to form the 43S preinitiation complex (reviewed in refs 1 and 2). Phosphorylation of the serine 51 residue in the α subunit of eIF2 promotes a complex formation between eIF2 and eIF2B, a rate-limiting heteropentameric guanine nucleotide exchange

(GNE) factor (3–6) and inhibits the GNE activity of eIF2B (7). These events lead to impairment in the recycling of eIF2 followed by inhibition of protein synthesis either globally or in a gene-specific manner (2, 8, 9). Abrogation of eIF2 α phosphorylation promotes transformation in NIH 3T3 cells (10), and eIF2 α phosphorylation levels increase in mammalian cells that are undergoing apoptosis (11), suggesting that a critical balance in eIF2 α phosphorylation is important for the survival or maintenance of cells in culture.

The four eIF2 α kinases identified and characterized so far phosphorylate the serine 51 residue in eIF2 α and share sequence and structural features that are distinguishable from other serine/threonine kinases. These are heme-regulated eIF2 α kinase (HRI), general control nonderepressible 2

[†] This work was supported by grants from CSIR (37/1120/02/EMR-II), New Delhi, India, to K.V.A.R., DST (4-1/2003-SF) to A.K.B., and DBT to S.E.H. G.A. acknowledges the support of a SRF fellowship from CSIR, New Delhi. A.K.B. is a recipient of the Swarnajayanti Award from DST, New Delhi.

* To whom correspondence should be addressed. Fax: 011-91-40-23010120, -23010451, or -23010145. E-mail: kvars1@uohyd.ernet.in.

[‡] Department of Biochemistry, University of Hyderabad.

[§] School of Chemistry, University of Hyderabad.

^{||} Laboratory of Molecular and Cellular Biology, CDFD.

[¶] National Institute of Immunology.

[¶] JNCASR.

[△] University of Michigan Medical Center.

¹ Abbreviations: eIF2 α , α subunit (38 kDa) of eukaryotic translational initiation factor 2; eIF2 α (P), phosphorylated eIF2 α ; Sf9, *Spodoptera frugiperda*; AcNPV, *Autographa californica* nuclear polyhedrosis virus; PERK, pancreatic endoplasmic-resident eIF2 α kinase; PKR, double-stranded RNA-dependent eIF2 α kinase; SDS–PAGE, sodium dodecyl sulfate–polyacrylamide gel electrophoresis; wt, wild type; Ac-DEVD-AFC, N-acetyl-Asp-Glu-Val-Asp-amino-4-(trifluoromethyl)coumarin; S51A eIF2 α , mutation of Ser51 eIF2 α to Ala; S51D eIF2 α , mutation of Ser51 eIF2 α to Asp; MoI, multiplicity of infection; z-VAD-fmk, carbobenzoxyvalylalanylasparyl(O-methyl) fluoromethyl ketone; PARP, poly(ADP-ribose) polymerase.

(GCN2) kinase that is activated upon amino acid starvation or accumulation of uncharged tRNAs (reviewed in ref 12), dsRNA-dependent protein kinase called PKR, and an endoplasmic-resident (ER) kinase called PEK or PERK that is activated during the accumulation of malformed proteins (reviewed in refs 2 and 13–16).

Induction of apoptosis in mammalian systems leads to changes in translational machinery that include cleavage of the 28S rRNA of the 60S subunit (17) and initiation factors such as eIF2 α (18, 19), eIF4B, eIF4GI, eIF4GII, and the j subunit of eIF3 (20–23). Additionally, apoptosis also alters the phosphorylation of translational initiation factors such as eIF2 α (11) and eIF4E BP1 (24) and various other cellular proteins (reviewed in ref 25). A recent study demonstrated caspase-dependent activation of PKR leading to eIF2 α phosphorylation during Fas-mediated apoptosis in Jurkat cells (26). PKR induces the activation of caspase-8 and/or other components of the signaling pathway involving TNF family receptors (27–29).

The ovarian cells of the lepidopteran insect *Spodoptera frugiperda* (*Sf9* and *Sf21*), natural hosts of baculovirus, have been extensively used to express recombinant proteins (30) and also as a model system for studying apoptosis (31–35). The significance of the present work is further augmented by the fact that both the death-ligand receptor pathway of apoptosis and PKR-mediated eIF2 α phosphorylation that are well-known in mammalian cells are unknown in insect cells. A specific baculovirus gene product, p35, was identified as being responsible for blocking the apoptotic response in host cells (33). The p35 protein, also called pancaspase inhibitor, prevents programmed cell death in phylogenetically diverse organisms such as *Caenorhabditis elegans*, *Drosophila melanogaster*, and humans (36–38). We previously showed that eIF2 α phosphorylation is reduced typically in wild-type virus-infected *Sf9* cells (3, 6). Further, expression of S51D (a phosphomimetic form of human eIF2 α in which the serine 51 residue is replaced by aspartic acid) in *Sf9* cells using recombinant baculovirus, although with reduced cell viability, did not induce apoptosis (3). However, the relationship between apoptosis and eIF2 α phosphorylation or phosphorylation of any other protein has not been demonstrated in *Sf9* cells.

The present study is undertaken to determine the importance of eIF2 α phosphorylation in mediating apoptosis in *Sf9* cells and to delineate the role of the antiapoptotic p35 baculovirus gene on eIF2 α phosphorylation. Our findings with a variety of pro- and nonapoptotic agents suggest that eIF2 α phosphorylation in *Sf9* cells need not always lead to apoptosis, but cells undergoing apoptosis are characterized by increased eIF2 α phosphorylation. Further, *Sf9* cells treated with a synthetic caspase inhibitor such as z-VAD-fmk or wt baculovirus infection resist apoptosis and show decreased eIF2 α phosphorylation, whereas infection of p35 mutant baculovirus leads to increased eIF2 α phosphorylation and apoptosis. The findings therefore suggest that the “pancaspase inhibitor” p35 protein produced by baculovirus mitigates eIF2 α phosphorylation and apoptosis. The mechanism of induction of eIF2 α phosphorylation in the presence of pro- and nonapoptotic agents appears to be different.

MATERIALS AND METHODS

Materials. A recombinant baculovirus vector harboring wt or S51A or S51D mutants of human eIF2 α was prepared from the parent vector pETFVA⁺ as described earlier (3, 6). A phosphospecific anti-eIF2 α antibody was obtained from Research Genetics, and polyclonal anti-eIF2 α was purchased from Santacruz Biotechnology Inc. Ac-DEVD-AFC, the substrate analogue of caspase(s), and recombinant human caspases-3 and -6 were purchased from BD Pharmingen. z-VAD-fmk, a cell-permeable caspase inhibitor, was obtained from Calbiochem. Glutathione–Sepharose 4B and BL21 cells were purchased from Amersham-Pharmacia. Mutant p35 virus, δ p35AcNPV, was obtained originally by one of us (S.E.H., CDFD, Hyderabad) from Dr. Paul D. Friesen’s laboratory in the Institute of Virology, University of Wisconsin, Madison, WI. Bovine PARP was obtained from Calbiochem, and the anti-PARP p85 fragment antibody was obtained from Promega, Inc.

Cell Culture. *S. frugiperda* (*Sf9*) cells were grown in TNM-FH medium supplemented with 10% fetal calf serum and antibiotics as described earlier (3, 32). Confluent cells with >95% viability were used in all experiments. The trypan blue exclusion test was carried out to assess the viability of the cells.

Induction of Apoptosis. *Sf9* cells were irradiated with UVB light (312 nm) for 30–60 s as described earlier (32) and incubated at 27 °C for 15 h or treated for 15 h with different agents such as etoposide, cycloheximide, EGTA, A23187, and tunicamycin. Apoptosis was also studied in the presence of a cell-permeable z-VAD-fmk, a caspase inhibitor, with wt AcNPV and with p35 deletion mutant virus (32). To evaluate the importance of eIF2 α phosphorylation in apoptosis, cells were treated with UVB radiation before and after the expression of wt and mutants of human eIF2 α . Expression of recombinant eIF2 α wt and mutants was carried out using a recombinant baculovirus as described earlier (3, 6).

Assays for Apoptosis. A total of 4×10^6 cells were taken for each experiment and scored for apoptosis by monitoring plasma membrane blebbing. A small aliquot, 45 μ L of cell suspension, was stained with 0.04% trypan blue and viewed under an inverted microscope (Labovet) equipped with a digital camera and the software MV500 DEMO to score (20 \times magnification) the apoptosed cells. Caspase activity of the cells undergoing apoptosis was determined using Ac-DEVD-AFC hydrolysis in the cell extracts as described (39). Approximately, 400 μ g of extract protein was taken in 50 μ L of extract buffer and was diluted to 750 μ L with 20 mM Tris-HCl buffer (pH 7.2) containing 1 mM Mg²⁺, 80 mM KCl, and 1 mM DTT for each reaction. Ac-DEVD-AFC hydrolysis was monitored by fluorescence emission of the released AFC (excitation, 400 nm; emission, 500 nm) using a Fluoromax-3, Jobin Yvon, Horiba spectrofluorometer as described earlier (39). The final concentration of Ac-DEVD-AFC used in the reactions was 10.9 μ M. Phosphorylation of eIF2 α in cell extracts containing 25 μ g of protein was monitored using a phosphospecific anti-eIF2 α antibody. Blots were scanned at a resolution of 200 dpi by using a Hewlett-Packard Scanjet 3400C. Band intensities were quantified using the Quantity Image Analysis software using a Bio-Rad Model GS-800 calibrated imaging densitometer.

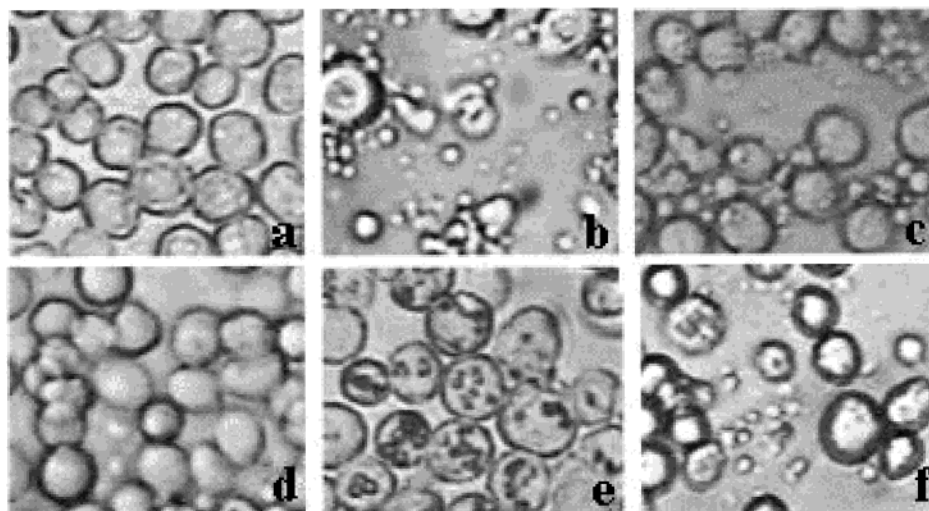


FIGURE 1: Apoptosis in *Sf9* cells. Cells were treated with the UVB light for 1 min as described earlier (32) and incubated for 15 h or with different agents for 15 h at 27 °C. Apoptosis was scored by microscopic observation as described under Materials and Methods. Magnification: 20 \times . Panels: a, uninfected cells; b, UVB-treated cells; c, etoposide-treated (125 μ M) cells; d, tunicamycin-treated (20 μ M) cells; e, wt AcNPV-infected cells treated with UVB radiation; f, p35 mutant virus-infected cells.

PARP Cleavage. In addition to monitoring the cell morphology and caspase activity of the cells undergoing apoptosis, the relative induction of apoptosis caused by various treatments was also studied by the cleavage of pure bovine poly(ADP-ribose) polymerase protein (PARP). Pure bovine PARP protein (150 ng) was incubated with the *Sf9* extracts (containing 60 μ g of protein) at 30 °C for 90 min in a 40 μ L reaction mixture consisting of 10 mM Tris-HCl, pH 7.5, 2.5 mM KH_2PO_4 , 2 mM NaCl, 68 mM sucrose, and 220 mM mannitol. The PARP reactions were processed by the addition of equal volume of 2 \times reducing buffer containing 62.5 mM Tris-HCl, pH 6.8, 6 M urea, 10% glycerol, 2% SDS, 5% β -mercaptoethanol, and 0.005% bromophenol blue. The PARP reaction samples were boiled at 65 °C for 15 min, then separated on 10% SDS-PAGE, transferred to a nitrocellulose membrane, and probed with an antibody (anti-rabbit antibody) that recognizes the 89 kDa cleaved fragment of PARP.

RESULTS

Pro- and Nonapoptotic Stresses. To elicit apoptosis, uninfected and baculovirus-infected *Sf9* cells were treated with DNA damaging agents such as UVB light, etoposide (DNA damaging agent), cycloheximide (a translational elongation inhibitor), EGTA (a calcium chelator), calcium ionophore, and tunicamycin (a N-linked glycosylation inhibitor) which are known to promote apoptosis in many mammalian systems. Cells were assayed for apoptosis by the trypan blue exclusion test, formation of apoptotic bodies, and caspase activation. Live and apoptotic cells excluded trypan blue. Apoptosis was assessed then by counting the live cells under the microscope that are distinctly larger than apoptotic bodies under higher magnification. The morphology of the cells undergoing apoptosis in the presence of UVB and etoposide is shown in Figure 1b,c. UVB treatment produced a maximum of 80–85% apoptotic bodies compared to the untreated controls (Figure 1b vs Figure 1a). A short exposure of UVB light for 30 s also resulted in 50–60% apoptosis (data not shown). We then compared the percent of apoptosis that occurred in the presence of different

concentrations of various other agents such as etoposide (20 and 125 μ M), cycloheximide (0.02, 0.5, and 3.0 mM), EGTA (10 and 50 mM), calcium ionophore A23187 (20 and 100 μ M), and tunicamycin (4 and 20 μ M). Of these agents, UVB was the most potent inducer of apoptosis (80–85%) followed by high concentrations of EGTA, etoposide, and cycloheximide (60–70% apoptosis). In contrast, high concentrations of tunicamycin (Figure 1d) and the calcium ionophore A23187 (data not shown), which were known to induce apoptosis in mammalian systems, produced very little or mild (5–10%) apoptosis. To monitor the effect of viral infection on the ability of these agents to induce apoptosis, *Sf9* cells were infected with baculovirus and then treated with some of these apoptotic agents. Baculovirus-infected cells can be recognized from uninfected *Sf9* cells by the presence of dark opaque polyhedral inclusion bodies under a light microscope. Wild-type virus-infected cells showed little or no apoptosis even after the treatment with proapoptotic agents such as UVB (Figure 1e). In contrast, a mutant virus that had a deletion of its p35 antiapoptotic gene promoted apoptosis (Figure 1f). Incubation of uninfected cells with the proapoptotic agents along with cell-permeable z-VAD-fmk, a caspase-3 inhibitor, resulted in almost total loss of apoptosis in these cells, and the morphology of these cells resembled that of the control *Sf9* cells (data not shown). These results thus indicate that not all stresses would lead to apoptosis. While UVB light, etoposide, cycloheximide (high concentrations), and EGTA were found to be proapoptotic agents, the calcium ionophore A23187 and tunicamycin were nonapoptotic. *Sf9* cells treated with baculovirus resist apoptosis presumably because of the expression of p35 protein, which is well-known as a caspase inhibitor.

Proapoptotic Agents Stimulate Caspase Activity. Since caspase activation is a characteristic event of cells undergoing apoptosis, the action of the above proapoptotic agents was monitored in terms of caspase activity in *Sf9* cells. The activity was measured in extracts of apoptotic cells by monitoring the hydrolysis of Ac-DEVD-AFC, a substrate specific for mammalian caspase-3 (Figure 2A). Little or no caspase activity was detected in uninfected control cell

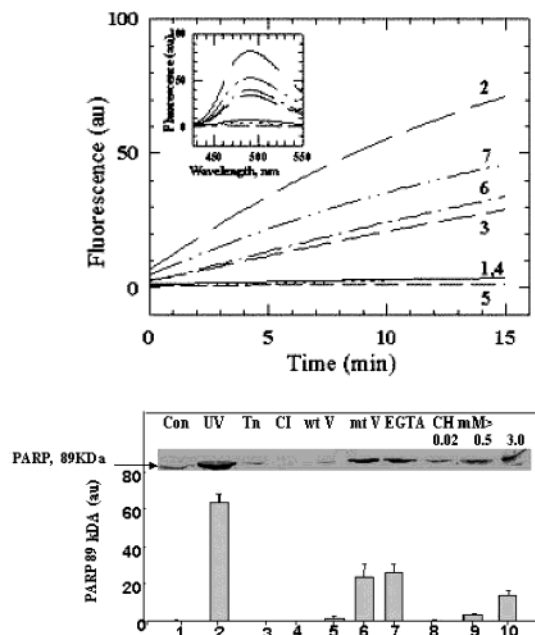


FIGURE 2: (A) Caspase activity in *Sf9* cell extracts. Cells were treated with various agents, and the caspase activity of the extracts was measured by using Ac-DEVD-AFC as described under Materials and Methods. Inset: Fluorescence spectrum recorded 20 min after addition of Ac-DEVD-AFC to the extracts. Curves 1–7 represent caspase activity in cells treated with the following agents: 1, control; 2, UVB; 3, 125 μ M etoposide; 4, 20 μ M cycloheximide; 5, 500 μ M cycloheximide; 6, 3.0 mM cycloheximide; 7, 50 mM EGTA. (B) PARP cleavage activity of *Sf9* cell extracts. The extracts were prepared from cells treated with various agents as follows. In the case of virus infection, *Sf9* cells were infected with wt baculovirus or p35 deletion mutant virus for 48 h before the extracts were made. In the case of UV treatment, cells were treated for 60 min with UVB light and then incubated for 15 h at 26 $^{\circ}$ C. All other treatments were carried out at 26 $^{\circ}$ C for 15 h. Cell extracts (\sim 60 μ g of protein) were then incubated with \sim 150 ng of purified bovine PARP at 30 $^{\circ}$ C for 90 min in the cleavage buffer described under Materials and Methods. The reactions were terminated and separated on 10% SDS–PAGE, transferred to a nitrocellulose membrane, and probed with an anti-PARP p85 fragment antibody. The figure is a western blot. The lanes are labeled as follows: 1, control; 2, UVB; 3, tunicamycin, 20 μ M; 4, A23187, 100 μ M; 5, wt AcNPV infection; 6, p35 deletion mutant AcNPV infection; 7, EGTA, 50 mM; 8, cycloheximide, 20 μ M; 9, cycloheximide, 500 μ M; 10, cycloheximide, 3 mM. The bar diagram below the blot represents average values of two independent experiments.

extracts (curve 1). Significant caspase activity was detected in uninfected cells treated with UVB light (curve 2), 50 mM EGTA (curve 7), 3 mM cycloheximide (curve 6), and 125 μ M etoposide (curve 3). Low concentrations of cycloheximide (20 and 500 μ M), however, did not activate caspase (curves 4 and 5). High concentrations (1.0–3.0 mM) of cycloheximide stimulated apoptosis and caspase activity. A marginal increase in caspase activity was observed in the presence of low and high concentrations of tunicamycin (4 and 20 μ M) and calcium ionophore (20 and 100 μ M) and is consistent with their inability to induce apoptosis (data not shown). Overall, caspase activity was found to be directly related to the level of apoptosis (Figure 2A).

PARP Cleavage. In addition to measuring the caspase activity by using Ac-DEVD-AFC hydrolysis, the relative levels of apoptosis observed under the microscope were further determined by studying PARP cleavage. Many earlier studies have shown that PARP is selectively cleaved by

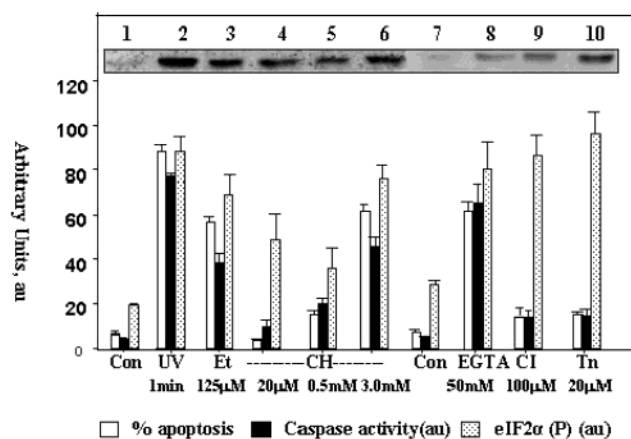


FIGURE 3: Status of eIF2 α phosphorylation, caspase activity, and apoptosis in uninfected *Sf9* cells as a function of treatment with different agents. Labels 1 and 7 represent two controls and are used to obtain relative changes in various activities as depicted in the bar diagram below for various treatments represented in labels 2–6 and 8–10, respectively. The bar diagram represents average values of three independent experiments. The treatments are as follows: 2, UVB for 60 s; 3, etoposide (Et), 125 μ M; 4, cycloheximide (CH), 20 μ M; 5, CH, 500 μ M; 6, CH, 3 mM; 8, EGTA, 50 mM; 9, calcium ionophore (CI), 100 μ M; 10, tunicamycin (Tn), 20 μ M. The top insert represents the status of eIF2 α phosphorylation as a function of different treatments. The western blot was scanned with a densitometer, and values were plotted in the form of a bar diagram depicting the various changes. The different bars show the extent of changes in percent or arbitrary units for percent apoptosis (open bars), caspase activity (filled bars), and eIF2 α phosphorylation (dotted bars).

several caspases, especially by caspase-3. Caspase-3 cleaves the 113 kDa PARP at the DEVD site between Asp214 and Gly215 to generate 89 and 24 kDa polypeptides. The cleavage of PARP here was measured by monitoring the appearance of the 89 kDa fragment of PARP that was recognized by an antibody (Figure 2B). The PARP cleavage was found to correlate the levels of apoptosis and caspase activation induced by various above agents (Figure 2A).

Pro- and Nonapoptotic Stresses Stimulate eIF2 α Phosphorylation in *Sf9* Cells. Phosphorylation of eIF2 α is a stress signal. All of the agents used here are known to stimulate eIF2 α phosphorylation in cultured mammalian cells. Further, eIF2 α phosphorylation has been shown to mediate apoptosis in mammalian cells (11). However, *Sf9* cells, despite their suitability as good model systems of apoptosis, have not so far been explored to determine the phosphorylation status of eIF2 or for that matter phosphorylation of any other protein in apoptotic and nonapoptotic stress conditions. The phosphorylation status of eIF2 α as a function of various treatments was determined here qualitatively and quantitatively using phosphospecific anti-eIF2 α antibody and compared with the extent of apoptosis and caspase activity for the respective treatments (Figure 3 bar diagram). The phosphospecific antibody was earlier shown to specifically recognize the phosphorylated form of eIF2 α not only in *Sf9* cell extracts but also from plant and mammalian cell types (3, 40). eIF2 α phosphorylation was enhanced significantly in uninfected *Sf9* cells in response to all of the agents tested (Figure 3) and is thus consistent with the notion that it is an indicator of stress. UVB treatment and higher concentration of tunicamycin (20 μ M) caused a maximum increase in eIF2 α phosphorylation (lanes 2 and 10). This was followed by calcium ionophore (100 μ M), EGTA (50 mM), cyclo-

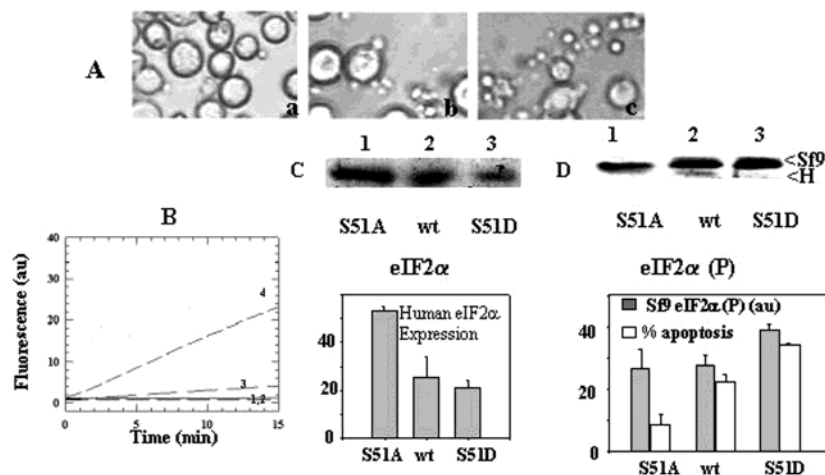


FIGURE 4: Apoptosis in UVB-treated *Sf9* cells expressing recombinant eIF2α wt and/or mutant proteins. Morphology of cells (panel A) treated first with UVB light for 60 s and then transfected with recombinant virus harboring human S51A (a), wt eIF2α (b), S51D (c) forms of eIF2α. Cells were analyzed after 48 h to estimate caspase activity (panel B), eIF2α expression (panel C), and phosphorylation (panel D). For caspase activity of *Sf9* cells (panel B) the curves are labeled as follows: 1, wt AcNPV; 2, UVB and recombinant virus harboring S51A eIF2α; 3, UVB and recombinant virus with wt eIF2α; 4, UVB and recombinant virus with S51D eIF2α. Panels C and D represent eIF2α expression and phosphorylation in UVB-treated *Sf9* cells using a polyclonal anti-eIF2α antibody and a phosphospecific anti-eIF2α antibody, respectively, as described under Materials and Methods. Lane labels are as follows: 1, cells expressing S51A mutant human eIF2α; 2, cells expressing wt eIF2α; 3, cells expressing S51D eIF2α. The bar diagrams below panels C and D represent average values of two independent experiments.

heximide (3 mM), and etoposide (125 μ M) (lanes 9, 8, 6, and 3, respectively). Both calcium ionophore and tunicamycin stimulated eIF2α phosphorylation (lanes 9 and 10) but failed to induce significant apoptosis. Similarly, low concentrations of cycloheximide (20 μ M) caused a substantial increase in eIF2α phosphorylation (lane 4) without inducing any apoptosis. An increase in the concentration of cycloheximide from 20 μ M to 0.5 mM, however, decreased eIF2α phosphorylation (lane 5). A further increase in the concentration of cycloheximide from 0.5 to 3.0 mM not only enhanced eIF2α phosphorylation (lane 6) but also induced apoptosis. A decrease in eIF2α phosphorylation between 0.02 and 0.5 mM cycloheximide may be due to the induction of a GAAD34-like protein that activates a protein phosphatase, PP1C (41). These results suggest that the type and magnitude of the stress play a role in eliciting apoptosis. Further, from a first glance of the data it appears as if there is no correlation between increased eIF2α phosphorylation and apoptosis. However, a close analysis of the results showed clear correlation among the three parameters that we have considered i.e., caspase activation, increased eIF2α phosphorylation, and apoptosis by various apoptotic agents. In contrast, the nonapoptotic agents stimulated eIF2α phosphorylation without apoptosis (Figure 3 bar diagram). These findings suggest that the mechanism of induction of eIF2α phosphorylation in apoptotic and nonapoptotic conditions is different.

eIF2α Phosphorylation Mediates Apoptosis in *Sf9* Cells. The importance of eIF2α phosphorylation in apoptosis and in nonapoptotic conditions or during translational inhibition caused by diverse conditions/agents in mammalian systems was analyzed previously by overexpressing a nonphosphorylatable form of eIF2α such as S51A (the serine 51 residue is replaced by alanine) or a phosphomimetic form of eIF2α, S51D (serine residue in position 51 is replaced by aspartic acid). While expression of S51A decreased both translational inhibition in heat-shocked mammalian cells (42) and apoptosis (11), S51D was found to stimulate these processes. To

determine the influence of eIF2α phosphorylation on apoptosis in *Sf9* cells, we expressed human wt and the S51A and S51D mutants of eIF2α using recombinant baculoviruses as described earlier (3). Overexpression of the recombinant human phosphomimetic form of eIF2α (S51D) did not promote apoptosis in *Sf9* cells in the absence of UVB exposure (data not shown). Also, *Sf9* cells infected with wt virus or recombinant S51D virus were unable to undergo apoptosis in response to UVB irradiation (data not shown). This is likely a reflection of the expression of antiapoptotic viral p35 protein that occurs during the early stages of viral infection. Consistent with this idea, apoptosis was found to be induced significantly in *Sf9* cells that were exposed first to UVB radiation and then transfected with recombinant virus harboring wt human eIF2α or S51D (Figure 4A, panels b and c). The S51D is a phosphomimetic form of eIF2α and therefore induced at least 30–35% higher apoptosis than the wild-type eIF2α (Figure 4A, panel b vs panel c). However, infection of *Sf9* cells with S51A virus carrying the nonphosphorylatable form of eIF2α resulted in a significant decrease in the UVB-induced apoptosis (Figure 4A, panel a). Caspase activity of these cells was related to apoptosis under those conditions (Figure 4B). No caspase activity was detected in cells pretreated with UVB and infected with wild-type baculovirus, AcNPV (Figure 4B, curve 1), as was the case with the recombinant virus harboring the S51A eIF2α (curve 2). In contrast, cells expressing the phosphomimetic S51D form of eIF2α showed a higher caspase activity compared to those carrying wild-type eIF2α (curves 4 and 3). The cell extracts were also analyzed to determine the expression of human eIF2α protein (Figure 4C) and also the phosphorylation status of the endogenous *Sf9* eIF2α and of the recombinant wt and mutant human eIF2α (Figure 4D). The expression of recombinant eIF2α wt and mutant proteins was detected by a polyclonal anti-eIF2α antibody that recognizes the human protein but not the endogenous *Sf9* protein (Figure 4C). Cells infected with the S51D mutant virus showed relatively lesser expression of the eIF2α protein than the

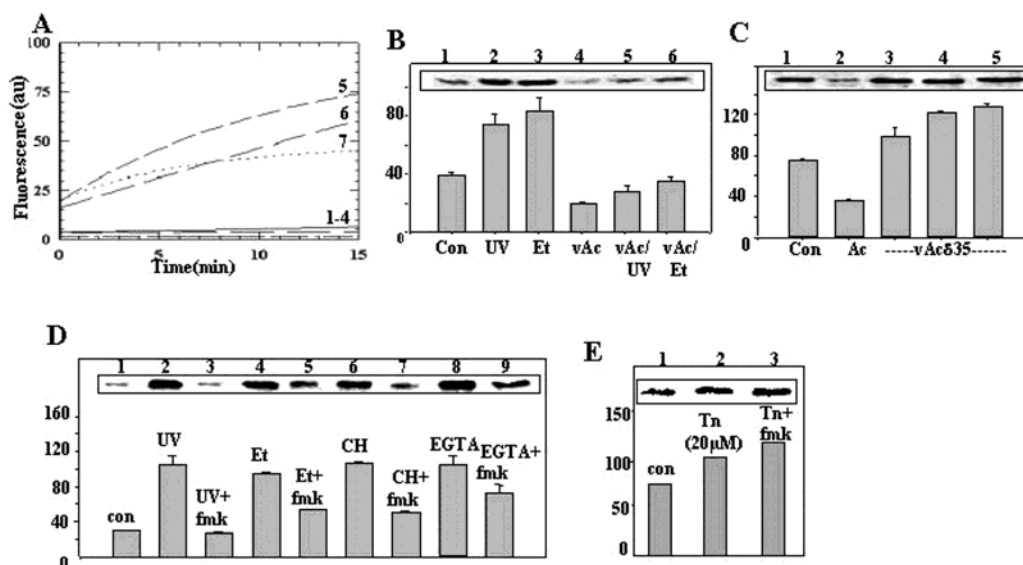


FIGURE 5: (A) Caspase activity in wt and p35 mutant baculovirus-infected extracts. Ac-DEVD-AFC hydrolysis in the extracts was measured as described in the legend to Figure 2 under the following conditions: 1, uninfected cells; 2, wt AcNPV-infected cells; 3, wt AcNPV-infected UVB-treated (1 min) cells; 4, wt AcNPV-infected etoposide-treated (125 μ M) cells; 5, UVB-treated uninfected cells; 6, etoposide-treated uninfected cells; 7, p35 mutant virus-infected cells. Panels B–E represent eIF2 α phosphorylation in extracts prepared from cells treated with various agents described below. Corresponding bar diagrams represent changes in phosphorylation in arbitrary units (au). The bar diagrams represent average values of two independent experiments. Panel B: lane 1, uninfected; lane 2, UVB-treated (60 s); lane 3, etoposide-treated (Et, 125 μ M); lane 4, wt AcNPV-infected (vAc); lane 5, vAc-infected and UV; lane 6, vAc-infected and etoposide-treated. Panel C: lane 1, uninfected; lane 2, wt AcNPV-infected; lanes 3–5, p35 deletion mutant virus (vAc δ 35) infected cell extracts with increasing virus titer. Panel D: lane 1, uninfected control; lane 2, UV-treated; lane 3, UVB + 50 μ M z-VAD-fmk; lane 4, 125 μ M etoposide; lane 5, 125 μ M etoposide + 50 μ M z-VAD-fmk; lane 6, 3 mM cycloheximide (CH); lane 7, 3 mM cycloheximide + 50 μ M z-VAD-fmk; lane 8, 50 mM EGTA; lane 9, 50 mM EGTA-treated + 50 μ M z-VAD-fmk. Panel E: lane 1, uninfected control; lane 2, 20 μ M tunicamycin (Tn); lane 3, 20 μ M tunicamycin + 50 μ M z-VAD-fmk.

S51A mutant virus (lane 3 vs lanes 1 and 2). We observed this earlier also (3), and it is a reflection of the toxic nature of the phosphomimetic form of S51D. A duplicate blot was probed with the phosphospecific antibody that recognizes both the human and *Sf9* proteins but only their phosphorylated forms (Figure 4D). Two bands were detected by the phosphospecific anti-eIF2 α antibody; the one with reduced mobility corresponds to *Sf9* eIF2 α , and the other one with increased mobility corresponds to the recombinant human eIF2 α (Figure 4D). Apoptosis induced by UVB was high in cells expressing the S51D eIF2 α mutant followed by the wt eIF2 α . This was also reflected in the phosphorylation status of endogenous eIF2 α (Figure 4D, lanes 2 vs 3, *Sf9* arrowhead). The cells expressing the S51A mutant of eIF2 α showed the least apoptosis with correspondingly reduced *Sf9* eIF2 α phosphorylation (Figure 4D, lane 1). The phosphorylation of recombinant human wt eIF2 α was evident in insect cells but not in the S51A and S51D mutants (Figure 4D, lower band, H arrowhead). These results suggest that phosphorylation of eIF2 α that occurs during apoptosis as a function of UVB exposure is likely due to caspase activation.

p35 Deletion Mutant Baculovirus Stimulates eIF2 α Phosphorylation and Promotes Apoptosis in *Sf9* Cells. Baculovirus infection of insect cells has been shown to decrease caspase activity and apoptosis (33). In accordance with earlier reports, caspase activity was barely detected, if at all, in *Sf9* cells infected with the AcNPV or in virus-infected cells treated with UVB and etoposide (Figure 5A). The wild-type virus that is required for a productive infection causes a reduction in eIF2 α phosphorylation in *Sf9* cells as described by us earlier (3). We further observed that wt virus-infected cells resist apoptosis in the presence of proapoptotic agents.

Increase in eIF2 α phosphorylation as a function of apoptosis was observed more significantly in UVB- and etoposide- (125 μ M) treated uninfected cells than in wild-type virus-infected cells (Figure 5B, lanes 2 and 3 vs lanes 5 and 6, respectively). To determine the importance of caspase involvement in stimulating eIF2 α phosphorylation in cells undergoing apoptosis, we studied the effect of virus-encoded p35 gene expression on eIF2 α phosphorylation. This was carried out by infecting *Sf9* cells with a deletion mutant p35 virus. Deletion mutant virus infection readily resulted in apoptosis (Figure 1f), caspase activity (Figure 5A, curve 7), and enhanced eIF2 α phosphorylation (Figure 5C, lanes 3–5).

Inhibition of Caspase Activity Mitigates eIF2 α Phosphorylation. Complementing the above results, eIF2 α phosphorylation and apoptosis (data not shown) were reduced in *Sf9* cells treated with z-VAD-fmk and then exposed to UVB (1 min), etoposide (125 μ M), cycloheximide (3.0 mM), and EGTA (50 mM) (Figure 5D, lanes 2, 4, 6, and 8 without inhibitor vs lanes 3, 5, 7, and 9 with inhibitor). Interestingly, tunicamycin-induced eIF2 α phosphorylation was not affected in the presence of z-VAD-fmk (Figure 5E, lanes 2 and 3 vs lane 1). This finding complements the observation on the inability of tunicamycin to stimulate caspase activity and apoptosis (Figure 3 bar diagram) and suggests that tunicamycin-induced eIF2 α phosphorylation is different from the increased eIF2 α phosphorylation caused by the addition of apoptotic agents in *Sf9* cells. These results therefore suggest that increased eIF2 α phosphorylation in apoptosis is a consequence of increased caspase activity.

Caspase Activation Occurs Prior to Enhanced eIF2 α Phosphorylation in UV-Induced Apoptosis. The kinetics of caspase activation and eIF2 α phosphorylation in UV-induced

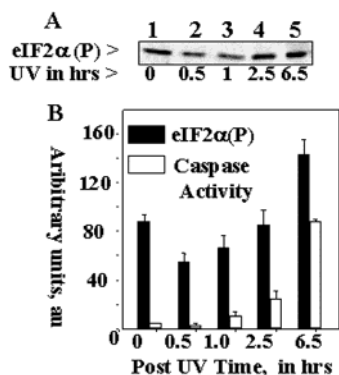


FIGURE 6: Kinetics of eIF2 α phosphorylation and caspase activation in UV-induced apoptosis in *Sf9* cells. Panel A represents eIF2 α phosphorylation as judged by a phosphospecific antibody at different time periods of UV-treated *Sf9* cells. The figure is a western blot. Lane labels are as follows: 1, control; 2–5, cell extracts prepared after 0.5, 1, 2.5, and 6.5 h of UVB irradiation. Panel B represents a bar diagram of an average of three independent experiments showing the relative densities of phosphorylated eIF2 α levels and caspase activity of UV-induced apoptotic cells at different time periods. Filled and open bars represent phosphorylation and caspase activity, respectively.

apoptotic cells indicate that caspase activation occurs around 1.0 h after UV treatment (Figure 6B bar diagram, bar 3 vs bar 1). The phosphorylation of eIF2 α was found to be decreased initially before the onset of caspase activation. However, the phosphorylation of eIF2 α was found to be increased 2.5 h after UV treatment (Figure 6A, lanes 4 and 5 vs lane 1 and the corresponding bar diagram). The maximum increase in eIF2 α phosphorylation was observed 15 h after treatment (as shown in Figures 3 and 5B,D) while the maximum caspase activation occurs around 6–8 h (Figure 6B bar diagram). These results together with the earlier results in Figure 5 indicate that caspase activation occurs prior to increased eIF2 α phosphorylation and is a prerequisite for the increased eIF2 α phosphorylation observed in cells that are undergoing apoptosis.

DISCUSSION

A major observation of this study is that uninfected, but not the wt AcNPV-infected, *Sf9* cells are very sensitive and respond to different signals by altering the phosphorylation status of cellular eIF2 α . We demonstrate that, in addition to UVB light and etoposide, higher concentrations of cycloheximide and EGTA promote apoptosis (Figures 1 and 3) and stimulate the caspase activity (Figure 2) and also eIF2 α phosphorylation in uninfected *Sf9* cells (Figure 3). In contrast, tunicamycin, A23187, and low concentrations of cycloheximide fail to activate caspase and consequent apoptosis (Figures 1–3). Nevertheless, these agents do stimulate eIF2 α phosphorylation in *Sf9* cells (Figure 3), suggesting that the stress signaling pathway is important in the induction of apoptosis. In addition, we have demonstrated that p35 mutant virus promotes apoptosis readily and stimulates eIF2 α phosphorylation in *Sf9* cells.

The mechanism of activation of caspases in *Sf9* cells vis-à-vis the role of p35 in inhibiting the maturation of caspase(s) is not well understood. It has been proposed that an unidentified apical caspase cleaves the pro-*Sf*-caspase-1 to p25 and p12, and subsequently the p25 caspase product gives rise to p19 (34). While cellular IAPs block the activation of

an apical unidentified caspase and inhibit the cleavage of Pro-*Sf*-caspase-1 to p25 and p12 products, baculovirus p35 blocks the cleavage of p25 caspase to p19, thereby inhibiting the maturation of caspase(s). This is further substantiated by the fact that apoptosis in insect cells, induced by UVB radiation and p35 deletion virus infection, is prevented by pro-*Sf*-caspase-1 inhibitors (34). We show here that p35 viral protein not only inhibits the formation of an active caspase and consequent apoptosis but also mitigates eIF2 α phosphorylation in *Sf9* cells (Figure 5A,C).

The importance of baculovirus p35-mediated caspase inhibition leading to diminished eIF2 α phosphorylation is substantiated further by the observation that wt virus-infected *Sf9* cells are unable to undergo apoptosis in response to UVB irradiation (Figure 1) or through the overexpression of the phosphomimetic form of eIF2 α (data not shown). On the contrary, apoptosis is stimulated readily in *Sf9* cells that are exposed first to UVB light and then transfected with the recombinant baculovirus carrying the phosphomimetic form of eIF2 α than with wt or the nonphosphorylatable form of eIF2 α (Figure 4). These observations in *Sf9* cells indicate that eIF2 α phosphorylation alone does not stimulate apoptosis or caspase activity, but it can enhance the apoptotic effect of caspase, suggesting thereby that eIF2 α phosphorylation is necessary but not a sufficient condition for the induction of apoptosis. The importance of increased eIF2 α phosphorylation as a function of increased caspase activity was further reinforced by using a cell-permeable inhibitor, z-VAD-fmk. The inhibitor decreases eIF2 α phosphorylation in cells exposed to proapoptotic agents such as UVB and etoposide and high concentrations of cycloheximide and EGTA (Figure 5D). In contrast, tunicamycin-induced eIF2 α phosphorylation was not affected by the presence of the caspase inhibitor (Figure 5E), which is found to be consistent with its inability to stimulate caspase activity or apoptosis. These findings also suggest that caspase activation is a prerequisite for increased eIF2 α phosphorylation in apoptotic cells. Consistent with these observations, an analysis of the kinetics of eIF2 α phosphorylation and caspase activation in UV-induced apoptotic cells indicates that caspase activation occurs prior to increased eIF2 α phosphorylation (Figure 6). In addition, we have also observed that recombinant eIF2 α kinases, such as mammalian PKR and PERK, are cleaved in vitro by cell-free extracts prepared from apoptosed *Sf9* cells and by purified caspase-3 (data not shown). Furthermore, caspase-3-treated PERK, when compared to caspase or PERK alone, can stimulate eIF2 α phosphorylation in extracts prepared from healthy insect cells (data not shown). The mechanism of eIF2 α phosphorylation observed in cells undergoing apoptosis thus appears to be different from the increased eIF2 α phosphorylation that occurs in response to various nonapoptotic stress conditions. These interpretations also find support from a recent study that demonstrated caspase-dependent PKR activation and eIF2 α phosphorylation (26). This notion that eIF2 α phosphorylation can be stimulated by an active eIF2 α kinase or active caspase draws further support from the viral proteins which can inhibit eIF2 α phosphorylation either by inactivation of the eIF2 α kinase (46) or by inhibition of maturation of caspases as has been shown here. Caspases are also known to process and enzymatically activate other kinases that include MEK

kinase-1 (MEKK-1), protein kinase C- δ , (PKC- δ), and p21 activated kinase-2 (PAK2) (45).

Interestingly, many viruses are known to produce proteins that interfere with PKR-mediated activation and inhibit host cell eIF2 α phosphorylation (46). A recent study has shown that baculovirus produces PK2 protein that resembles the C-terminal half of a protein kinase domain and is found to inhibit activation of GCN2, PKR, and HRI eIF2 α kinases in vitro (47). It is not known, however, if PK2 interferes with the host apoptosis. Our findings here suggest that baculovirus-coded p35, an antiapoptotic or a caspase inhibitor protein, interferes with the activation of host cell eIF2 α kinase, albeit indirectly through the inactivation of a host cell caspase. Despite suggestions by Blair et al. (48) that *Sf9* cells contain a protein that is antigenically related to PKR, PKR-encoding sequences have not been recognized in any invertebrate for which the complete genome sequence is available. Also, the eIF2 α kinases present in *Sf9* insect cells have not been characterized, although GCN2 and PERK have been characterized in *Drosophila* (43, 44). Since agents such as UVB light, cycloheximide, EGTA, A23187, tunicamycin, and DNA damaging agents are known to stimulate unfolded protein response (UPR) or stress in the endoplasmic reticulum (ER) (49–52), it is likely that *Sf9* cells have an ER-resident eIF2 α kinase-like PERK which is stimulated in response to all of these agents as evidenced by increased eIF2 α phosphorylation. The activation of PERK or other eIF2 α kinases by an active caspase is obviously essential to promote apoptosis.

Phosphorylation of eIF2 α is known to inhibit translation of several mRNAs leading to a decline in protein synthesis globally (53). Paradoxically, the translation of transcriptional factors such as GCN4 (general control nonderepressible) in yeast and ATF4 (activated transcription factor) in mammalian systems is increased in response to eIF2 α phosphorylation (reviewed in refs 54 and 57). Although tunicamycin and the calcium ionophore are known to cause ER stress and promote apoptosis in mammalian systems, these agents did not induce apoptosis here in *Sf9* cells. This may be related to the type and magnitude of the stress, the physiological response of the cells toward each of these stress conditions, and also the cell type (50). Further, most of the work on ER stress signaling is carried out in mammalian systems, and very little is known in insect cells. In mammalian systems, cellular stress activates intracellular signaling pathways that affect a sizable number of transcriptional factors leading to alterations in the gene expression. ER is a repository for both pro- and antiapoptotic molecules. The activation of transcriptional factors such as ATF4, GCN4, and NF- κ B that occurs in response to ER stress, in turn, would stimulate the expression of several proapoptotic (CHOP/GADD-153) and prosurvival proteins including GADD 34, Bip/GRP78, calreticulin, protein disulfide isomerase, NF- κ B, etc. (51, 57). Posttranslational modifications of CHOP can lead to the transcriptional activation of novel stress-induced genes called DOC 6 and DOC 4 (downstream of CHOP) that share homology with the mammalian actin binding proteins such as villin and gelsolin or a mammalian orthologue of a *Drosophila* gene, *Tenm/Odz*, respectively. While Doc 6 is implicated in cell death, Doc 4 is important in cellular regeneration (56). Prolonged ER stress leads to cell death. Activation of ER-resident caspase-12 occurs by different mechanisms such as

the caspase-7/caspase-12 pathway and caspase 12/calpain pathway (58). A number of stimuli that disrupt protein folding such as tunicamycin and the calcium ionophore can activate both unfolded protein response (UPR) and ER overload response (EOR). These two signaling pathways respond to different and overlapping types of ER stresses, and their common feature for their induction is not known (51). While UPR induces transcription of proapoptotic genes such as CHOP, EOR induces antiapoptotic genes such as NF- κ B (51). A recent study further describes that NF- κ B, an antiapoptotic protein, inhibits activation of GADD 153/CHOP in breast cancer cells exposed to tunicamycin or the calcium ionophore (50). It is likely that such paradoxical interactions of anti- and proapoptotic transcription factors in *Sf9* cells may be responsible for the specific differences in stress-induced apoptosis. The microdissection of the signaling events leading to stress-induced apoptosis in insect cells and the players involved in this process remain to be elucidated. Nonetheless, the degree of conservation in these processes between the vertebrates and the invertebrate systems renders *Sf9* insect cells an indispensable model system to study apoptosis.

REFERENCES

- Clemens, M. J. (1996) in *Translational Control* (Hershey, J. W. B., Mathews, M. B., and Sonenberg, N., Eds.) pp 139–172, Cold Spring Harbor Laboratory Press, Cold Spring Harbor, NY.
- Hinnebusch, A. G. (2000) in *Translational Control of Gene Expression* (Sonenberg, N., Hershey, J. W. B., and Mathews, M. B., Eds.) pp 185–243, Cold Spring Harbor Laboratory Press, Cold Spring Harbor, NY.
- Sudhakar, A., Ramachandran, A., Sudip, G., Hasnain, S. E., Kaufman, R. J., and Ramaiah, K. V. A. (2000) *Biochemistry* 39, 12929–12938.
- Krishnamoorthy, T., Pavitt, G. D., Zhang, F., Dever, T., and Hinnebusch, A. G. (2001) *Mol. Cell. Biol.* 21, 5018–5030.
- Pavitt, G. D., Ramaiah, K. V. A., Kimball, S. R., and Hinnebusch, A. G. (1998) *Genes Dev.* 12, 514–526.
- Sudhakar, A., Krishnamoorthy, T., Jain, A., Chatterjee, U., Hasnain, S. E., Kaufman, R. J., and Ramaiah, K. V. A. (1999) *Biochemistry* 38, 15398–15405.
- Ramaiah, K. V. A., Davies, M. V., Chen, J. J., and Kaufman, R. J. (1994) *Mol. Cell. Biol.* 14, 5018–5030.
- Jackson, R. J. (1991) in *Translation in eukaryotes* (Trachsel, H., Ed.) pp 93–229, CRC Press, Boca Raton, FL.
- Webb, B. L., and Proud, C. G. (1997) *Int. J. Biochem. Cell. Biol.* 10, 1127–1131.
- Donze, O., Jagus, R., Koromilas, A. E., Hershey, J. W. B., and Sonenberg, N. (1995) *EMBO J.* 14, 3828–3834.
- Srivastava, S. P., Kumar, K. U., and Kaufman, R. J. (1998) *J. Biol. Chem.* 273, 2416–2423.
- Dever, T. E. (1999) *Trends Biochem. Sci.* 24, 398–403.
- Chen, J. J., and London, I. M. (1995) *Trends Biochem. Sci.* 20, 105–108.
- Clemens, M. J., and Elia, A. (1997) *J. Interferon Cytokine Res.* 17, 503–524.
- Shi, Y., Vattam, K. M., Sood, R., An, J., Liang, J., Stramm, L., and Wek, R. C. (1998) *Mol. Cell. Biol.* 18, 7499–7509.
- Harding, H. P., Zhang, Y., and Ron, D. (1999) *Nature* 397, 271–274.
- Houge, G., Robaye, B., Eikhom, T. S., Golstein, J., Mellgren, G., Gjertsen, B. T., Lanotte, M., and Doskeland, S. O. (1995) *Mol. Cell. Biol.* 15, 2051–2062.
- Marissen, W. E., Guo, Y., Thomas, A. A., Matts, R. L., and Lloyd, R. E. (2000) *J. Biol. Chem.* 275, 9314–9323.
- Satoh, S., Hijikata, M., Handa, H., and Shimotohno, K. (1999) *Biochem. J.* 342, 65–70.
- Bushell, M., Poncet, D., Marissen, W. E., Flotow, H., Lloyd, R. E., Clemens, M. J., and Morley, S. J. (2000) *Cell Death Differ.* 7, 628–636.
- Bushell, M., Wood, W., Clemens, M. J., and Morley, S. J. (2000) *Eur. J. Biochem.* 267, 1083–1091.

22. Clemens, M. J., Bushell, M., and Morley, S. J. (1998) *Oncogene* 17, 2921–2931.
23. Clemens, M. J., Bushell, M., Jeffrey, I. W., Pain, V. M., and Morley, S. J. (2000) *Cell Death Differ.* 7, 603–615.
24. Tee, A. R., and Proud, C. G. (2002) *Mol. Cell. Biol.* 22, 1674–1683.
25. Fischer, U., Janicke, R. U., and Schulze-Osthoff, K. (2003) *Cell Death Differ.* 10, 76–100.
26. Saelens, X., Kalai, M., and Vandenabeele, P. (2001) *J. Biol. Chem.* 276, 41620–41628.
27. Balachandran, S., Kim, C. N., Yeh, W., Mak, T. W., Bhalla, K., and Barber, G. N. (1998) *EMBO J.* 17, 6888–6902.
28. Gil, J., and Esteban, M. (2000) *Oncogene* 19, 3665–3674.
29. Jeffrey, I. W., Bushell, M., Tilleray, V. J., Morley, S., and Clemens, M. J. (2002) *Cancer Res.* 62, 2272–2280.
30. Luckow, V. A., and Summers, M. D. (1988) *Virology* 167, 56–71.
31. Hasnain, S. E., Taneja, T. K., Sah, N. K., Mohan, M., Pathak, N., Sahdev, S., Athar, M., Totey, S. M., and Begum, R. (1999) *J. Biosci.* 24, 13–18.
32. Sah, N. K., Taneja, T. K., Pathak, N., Begum, R., Athar, M., and Hasnain, S. E. (1999) *Proc. Natl. Acad. Sci. U.S.A.* 96, 4838–4843.
33. Clem, R. J., Fechheimer, M., and Miller, L. K. (1991) *Science* 254, 1388–1390.
34. Manji, G. A., and Frieson, P. D. (2001) *J. Biol. Chem.* 276, 16704–16710.
35. Clem, R. J., and Miller, L. K. (1994) *Mol. Cell. Biol.* 14, 5212–5222.
36. Xue, D., and Horvitz, R. H. (1995) *Nature* 377, 248–251.
37. Hay, B. A., Wolff, T., and Rubin, G. M. (1994) *Development* 120, 2121–2129.
38. Beidler, D. R., Tewari, M., Frieson, P. D., Poirier, G., and Dixit, V. M. (1995) *J. Biol. Chem.* 270, 16526–16528.
39. Bhuyan, A. K., Varshney, A., and Mathew, M. K. (2001) *Cell Death Differ.* 8, 63–69.
40. Laxminarayana, B., Krishna, V. M., Janaki, N., and Ramaiah, K. V. A. (2002) *Arch. Biochem. Biophys.* 400, 85–96.
41. Novoa, I., Zeng, H., Harding, H. P., and Ron, D. (2001) *J. Cell Biol.* 153, 1011–1022.
42. Murtha-Riel, P., Davies, M. V., Scherer, B., Choi, S. Y., Hershey, J. W. B., and Kaufman, R. J. (1993) *J. Biol. Chem.* 268, 12946–12951.
43. Sood, R., Porter, A. C., Ma, K., Quilliam, L. A., and Wek, R. C. (2000) *Biochem. J.* 346, 281–293.
44. Berlanga, J. J., Santoyo, J., and De Haro, C. (1999) *Eur. J. Biochem.* 265, 754–762.
45. Widmann, C., Gibson, S., and Johnson, G. L. (1998) *J. Biol. Chem.* 273, 7141–7147.
46. Kaufman, R. J. (1999) *Proc. Natl. Acad. Sci. U.S.A.* 96, 11693–11695.
47. Dever, T. E., Sripriya, J. R., McLachlin, J., Lu, J., Fabian, R., Kimball, S. R., and Miller, L. K. (1998) *Proc. Natl. Acad. Sci. U.S.A.* 95, 4164–4169.
48. Blair, E. D., Roberts, C. M., Snowden, B. W., Gatignol, A., Benkirane, M., and Jeang, K. T. (1995) *J. Biomed. Sci.* 2, 322–329.
49. Wu, S., Hu, Y., Wang, J. L., Chatterjee, M., Shi, Y., and Kaufman, R. J. (2002) *J. Biol. Chem.* 277, 18077–18083.
50. Nozaki, S., Sledge, G. W., Jr., and Nakshtri, H. (2001) *Oncogene* 20, 2178–2185.
51. Kaufman, R. J. (1999) *Genes Dev.* 13, 1211–1233.
52. Williams, D. D., Pavitt, G. D., and Proud, C. G. (2001) *J. Biol. Chem.* 276, 3733–3742.
53. Mathews, M. B., Hunt, T., and Brayley, A. (1973) *Nat. New. Biol.* 243, 230–233.
54. Hinnebusch, A. G. (1996) in *Translational Control* (Hershey, J. W. B., Mathews, M. B., and Sonenberg, N., Eds.) pp 199–244, Cold Spring Harbor Laboratory Press, Cold Spring Harbor, NY.
55. Zinszner, H., Kuroda, M., Wang, X. Z., Batchvarova, N., Lightfoot, R. T., Remotti, H., Stevens, J. L., and Ron, D. (1998) *Genes Dev.* 12, 982–985.
56. Wang, X. Z., Kuroda, M., Sok, J., Batchvarova, N., Kimmel, R., Chung, P., Zinszner, H., and Ron, D. (1998) *EMBO J.* 17, 3619–3630.
57. Ron, D. (2003) *J. Clin. Invest.* 110, 1383–1388.
58. Rao, R. V., Castro-Obregon, S., Frankowski, H., Schuler, M., Stoka, V., Rio, G. D., Bredesen, D. E., and Ellerby, H. M. (2002) *J. Biol. Chem.* 277, 21836–21842.

BI0349423